

Periodic Anderson model with Holstein phonons for the description of the Cerium volume collapse

Enzhi Li^{1,2}, Shuxiang Yang^{1,2}, Peng Zhang³, Ka-Ming Tam^{1,2}, Mark Jarrell^{1,2}, and Juana Moreno^{1,2}

¹ Department of Physics & Astronomy, Louisiana State University, Baton Rouge, LA 70803, USA

² Center for Computation & Technology, Louisiana State University, Baton Rouge, LA 70803, USA and

³ Department of Physics, Xi'an Jiaotong University, Xi'an, Shaanxi, China

(Dated: March 2, 2022)

In order to better understand the effect of the electron-phonon interaction on the volume collapse transition of Cerium, we study the periodic Anderson model with coupling between Holstein phonons and electrons in the conduction band. We find that the electron-phonon coupling can enhance the volume collapse, which is consistent with experiments. Although we start with the Kondo Volume Collapse scenario in mind, our results capture some interesting features of the Mott scenario, such as a gap in the conduction electron spectra which grows with the effective electron-phonon coupling.

The isostructural volume collapse of Cerium is a long-standing puzzle [1]. When a crystal of Cerium is under a pressure of 15,000 atmospheres, it undergoes a volume collapse of approximately 17 percent while preserving the face-centered cubic crystal structure. This transformation, called the $\gamma \rightarrow \alpha$ transition, has baffled physicists since its discovery, and several leading theories have been proposed for its explanation, the most prominent of which are the Mott transition scenario [2] and the Kondo volume collapse (KVC) scenario [3]. The Mott and KVC scenarios are competing paradigms, although perhaps not as different and distinct as previously thought [4, 5].

In the KVC scenario, the $4f$ electrons of Cerium are assumed to be localized in both phases. In the small volume α phase, the spd electrons strongly screen the local moments of the f electrons, thus rendering the α phase a Pauli paramagnet. While in the large volume γ phase, the local moments of the f electrons persist to much lower temperatures than in the α phase, indicating that the Kondo scale T_K in the γ phase is much smaller than that of the α phase, which is consistent with the experimental observations [6–9].

In the Mott transition scenario, for which the Hubbard model is a good description, the density of states (DOS) of the f electrons changes from being metallic (no gap at the Fermi level) in the α phase to insulating (with a gap at the Fermi level) in the γ phase [5, 10–12]. This localization-delocalization of the $4f$ electrons, which is a metal-insulator Mott transition, is driven by the increase of the intersite hopping amplitudes of the f electrons when the unit cell volume of Cerium decreases.

Recent experimental and theoretical results have indicated that the electron-phonon interaction may also play an important role in the $\gamma \rightarrow \alpha$ transition [13–16]. Jeong *et al.* estimated that about one half of the entropy change during the transition is due to lattice vibrations. Later, Krisch *et al.* showed that the significant changes in the phonon dispersion across the $\gamma \rightarrow \alpha$ transition provide strong evidences for the importance of the lattice degrees of freedom. Although the precise value of the lattice vibrational entropy varies between experiments, they

do agree that a significant fraction of the total entropy change during the transition is due to lattice vibrations.

To test whether the electron-phonon interaction enhances the $\gamma \rightarrow \alpha$ transition, we consider a periodic Anderson model in which the conduction electrons are coupled to Holstein phonons [17]. Our model Hamiltonian is

$$\begin{aligned} \hat{H} &= \hat{H}_0 + \hat{H}_I \quad (1) \\ \hat{H}_0 &= -t \sum_{\langle i,j \rangle, \sigma} (c_{i,\sigma}^\dagger c_{j,\sigma} + c_{j,\sigma}^\dagger c_{i,\sigma}) + \epsilon_f \sum_{j,\sigma} f_{j,\sigma}^\dagger f_{j,\sigma} \\ &\quad + V \sum_{i,\sigma} (c_{i,\sigma}^\dagger f_{i,\sigma} + f_{i,\sigma}^\dagger c_{i,\sigma}) + \sum_i \left(\frac{P_i^2}{2m} + \frac{1}{2} k X_i^2 \right) \\ \hat{H}_I &= U \sum_i n_{i,\uparrow}^f n_{i,\downarrow}^f + g \sum_{i,\sigma} n_{i,\sigma}^c X_i. \end{aligned}$$

Here, $c_{i,\sigma}^\dagger, c_{i,\sigma} (f_{i,\sigma}^\dagger, f_{i,\sigma})$ creates and destroys a $c(f)$ electron of spin σ at lattice site i , respectively. P_i and X_i are the phonon momentum and displacement operators. Here, we have used dispersionless Einstein phonons with frequency $\Omega_0 = \sqrt{k/m}$. The parameter g measures the electron-phonon interaction strength, U is the Hubbard repulsion between localized f -electrons, and V characterizes the hybridization between c - and f -electrons. From the parameters g, k , we construct the effective electron-phonon interaction strength, $U_{eff} = \frac{g^2}{2k}$. Throughout this paper and to be consistent with the experimental results, we have set $\Omega_0 = 0.01$ [17] unless otherwise specified. We also set $U = 4$, the c -electron filling number to 0.8, and the f -electron filling number to 1.0.

We solve this model using the dynamical mean field theory [18], with the continuous time quantum Monte Carlo [19] as our impurity solver. We use a hypercubic lattice with Gaussian bare DOS, and consider its bandwidth as our unit of energy. We set this unit to be the Fermi energy ϵ_F of Cerium, which is 0.52eV [20, 21]. Finally, we use the maximum entropy method [22] to extract the spectral functions from the Monte Carlo simulation data.

We find that the first order phase transition emerges only when the electron-phonon interaction is large, which

justifies its introduction into our model. Although we employ the periodic Anderson model, the paradigm for the KVC scenario, our results display many features of a Mott transition. In the parameter regime where V is small, as U_{eff} increases, the DOS of the c -electrons gradually develops a gap at the Fermi level with a width proportional to U_{eff} . The gap-opening in the DOS, and its proportionality to U_{eff} are reminiscent of the Mott transition in the Hubbard model. Another issue that is noticeable is that the gap-opening does not occur when V dominates over U_{eff} , which compels us to argue that there is a competition between V and U_{eff} in our model [23].

Since the $\gamma \rightarrow \alpha$ transition is first order, the pressure versus volume curve develops a kink as the temperature drops below the transition point. To properly account for the static lattice contribution, we introduce a volume and temperature dependent bulk modulus term into our pressure-volume ($p - \mathcal{V}$) relation [3]. Therefore, the total pressure contains two parts, the pressure due to the electrons which we denote as p_e , and the pressure due to the bulk modulus term which we denote as p_B .

We calculate p_e from the electronic free energy by the relation $p_e = -\frac{\partial F}{\partial \mathcal{V}}$, and p_B by integrating the bulk modulus $B = -\mathcal{V}\frac{\partial p_B}{\partial \mathcal{V}}$. We calculate the electronic free energy using the formula $F_e(T = T_0, \mathcal{V} = \mathcal{V}_0, N) = \int_0^N \mu dN + F(T_0, \mathcal{V}_0, N = 0)$. Here, we choose not to use the entropy formula employed in Ref. [24] because the statistical error in our results become large at high temperatures. When we plot the free energy versus hybridization V , we notice that the curve continuously evolves from a nearly flat plateau at small V to a nearly straight line with a negative slope at large V . With this observation, we fit the free energy to the function

$$F_e(V) = -k\left(V - c + \frac{1}{a} \log 2 \cosh a(V - c)\right) + d. \quad (2)$$

By fitting our numerical data to Eq. [2], we obtain the values of the parameters k, a, c, d . Since the free energy depends on the temperature, these parameters also depend on it. Now, we can obtain the volume dependence of the free energy using the empirical relationship between hybridization V and volume \mathcal{V} , $V = \frac{b}{\mathcal{V}^2}$ [25]. We calculate the electronic pressure as

$$p_e = -\frac{2kb}{\mathcal{V}^3} \left(1 + \tanh a\left(\frac{b}{\mathcal{V}^2} - c\right)\right). \quad (3)$$

The experimental value of b can be estimated from the relation $V = \frac{b}{\mathcal{V}^2}$, and $J \propto \frac{V^2}{U}$ [26], where J is the Kondo exchange. The experimental values of J range between $0.2 - 0.3eV$ in the α phase and $0.05 - 0.06eV$ in the γ phase [6-8, 20]. From the values of J and the relation between J and the volume, we can estimate the value of b to be between 0.89 and 1.55 in our unit system.

The second contribution to the total pressure comes from the bulk modulus. From the experimental results

of Ref. [27, 28], we assume that the bulk modulus depends upon the volume as

$$B = B_0(T)e^{\alpha(1-\mathcal{V}/\mathcal{V}_0)}, \quad (4)$$

and upon the temperature through the relation [29]

$$B_0(T) = B_0(1 + e^{-\frac{T_0}{T}}), \quad (5)$$

where, B_0, T_0, \mathcal{V}_0 and α are material-dependent parameters.

Integration of the bulk modulus gives us the pressure p_B as

$$p_B(\mathcal{V}, T) = p_0(T) - B_0(T) \int_1^{\mathcal{V}/\mathcal{V}_0} dx \frac{e^{\alpha(1-x)}}{x}, \quad (6)$$

where p_0 is an arbitrary constant that may depend on the temperature. Throughout the paper, we have set $p_0 = 0$.

Adding the bulk modulus and the electronic pressures yields a $p - \mathcal{V}$ graph which exhibits a kink structure. Fig. 1 shows the pressure versus volume diagrams for different values of U_{eff} . When $U_{eff} = 1$, as we lower the temperature, a kink structure begins to develop. The crossing of the $p - \mathcal{V}$ diagrams at different temperatures may be removed once we retain the temperature dependence of the integration constants p_0 . Even if we set all the p_0 to 0, as we did in this paper, the crossing could still be a numerical artifact of our approximation, since the introduction of the volume dependence of the hopping amplitude t will make the $p - \mathcal{V}$ diagrams drop faster in the large volume regime, thus possibly eliminating this crossing feature.

On the other hand, when $U_{eff} = 0$ (inset on Fig. 1), even though we have used the same set of parameters, the kink structure that is the indicator for the emergence of a first order phase transition is absent. Note that the small upturn in the $p - \mathcal{V}$ diagram at large volume can also be eliminated once we consider the volume dependence for the hopping term t in the conduction band. The different behavior of the $p - \mathcal{V}$ diagram for $U_{eff} = 0$ and $U_{eff} = 1$ implies that the electron-phonon interaction enhances the $\gamma \rightarrow \alpha$ volume collapse transition.

Similar results can be obtained with many different combinations of parameters. In the data displayed in Fig. 1 we set $b = 1.18, p_0 = 0, T_0 = 0.1, B_0 = 12.47$, and $\alpha = 4.225$. The value of b is within our estimated range. A value of $T_0 = 0.1$ is approximately 600 K within our units, a value comparable to the critical point temperature of the transition. Following Ref. [3], we use $B_0 = 28GPa, \mathcal{V}_0 = 36\text{\AA}^3$ as the bulk modulus and unit cell volume for Cerium in the γ phase. Once we use the Fermi scale as our unit of energy and set \mathcal{V}_0 as our unit of volume, the unit of pressure becomes $\epsilon_F/\mathcal{V}_0 = 2.3GPa$. This justifies our usage of the value $B_0 = 12.47$ as our bare bulk modulus. And, finally, the experimental values of α range between 2 and 5 for most bulk pure metals [27].

This phonon-enhanced first order phase transition is actually a Mott metal-insulator transition which can be

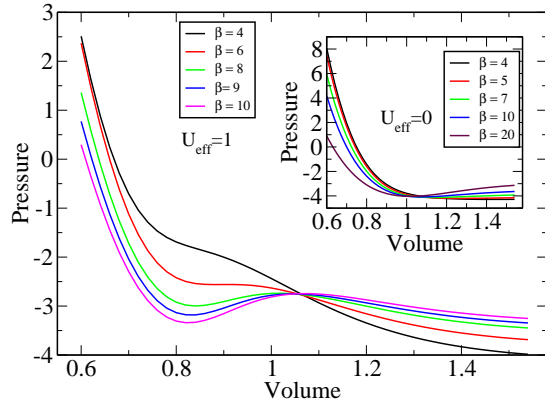


FIG. 1. Main panel: The $p(\text{pressure}) - \mathcal{V}(\text{volume})$ diagram for $U_{eff} = 1, \Omega_0 = 0.01$. As the temperature decreases, a kink structure develops in the $p - \mathcal{V}$ graph, indicating the emergence of a first order phase transition. Inset: $p - \mathcal{V}$ diagram for $U_{eff} = 0$. Here, with the same bulk modulus pressure, the kink structure does not show up.

better understood by studying the evolution of the spectral functions with respect to the variation of the relative strengths of V and U_{eff} . When the hybridization is small, the electron-phonon interaction can significantly modify the DOS of the conduction electrons. For $V = 0.1$, as U_{eff} increases from 0 to 1.1, the DOS changes from a nearly Gaussian to a DOS gapped at the Fermi energy, as shown in Fig. 2. We can also see the effect of U_{eff} on the gap at the Fermi energy by observing the behavior of the local c -electron Green's function $G_c(\tau)$. When there is no gap, the value of $G_c(\tau = \beta/2)$ is finite. However, when there is a gap at $\omega = 0$, the value of $G_c(\tau = \beta/2)$ decays to zero exponentially. Moreover, the wider the gap, the more rapid the decay. When we plot the $G_c(\tau)$ for different values of U_{eff} , we see clearly that with increasing U_{eff} , $G_c(\tau)$ decreases increasingly rapidly when τ approaches $\beta/2$.

The magnitude of the bare phonon frequency Ω_0 and the c -electron filling have profound influences on the nature of the Mott transition due to U_{eff} . When Ω_0 is small, which is the case we are studying, the transition seems to be continuous or at most extremely weakly discontinuous [30]. The reason is that when $\Omega_0 = 0$, we can integrate out the Holstein phonons to obtain the Falicov-Kimball model in which the conduction electrons always exhibit a non-Fermi liquid behavior for any non-trivial filling number [31, 32]. The Mott transition from a non-Fermi liquid metal to an insulator is continuous due to the absence of the quasi-particle peak at the Fermi energy in the conduction electron DOS [33]. On the other hand, when $\Omega_0 \rightarrow \infty$, the half-filling Holstein model exhibits a first order metal insulator phase transition at zero temperature [30]. It is however suggested that when doped away from half-filling, this first order phase transition

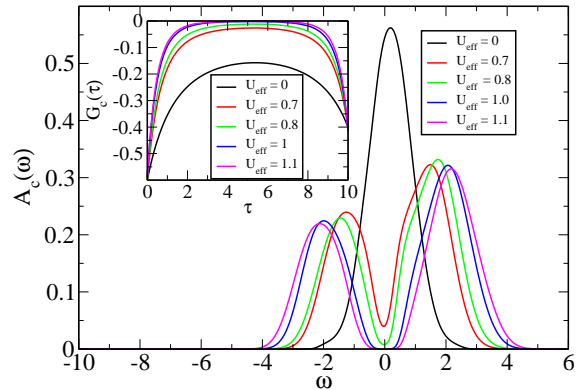


FIG. 2. Main panel: The conduction electron spectral functions for $V = 0.1, \beta = 10, \Omega_0 = 0.01$. As U_{eff} increases from 0.0 to 1.1, the gap in the DOS becomes increasingly wider. Inset: The evolution of the local conduction electron Green's function $G_c(\tau)$ with U_{eff} . The increasingly rapid decay of $G_c(\tau = \beta/2)$ also indicates the existence of an energy gap at $\omega = 0$ as U_{eff} grows.

may be strongly suppressed. Since we are doping our model away from half-filling, and the bare phonon frequency we are using is rather small, we do not expect to see a first order metal-insulator transition. The hitherto absence of a stable hysteresis loop in the $-\frac{1}{\pi} \text{Im}G_c(i\pi T)$ versus U_{eff} plane for varying values of Ω_0 at finite temperature may provide support for this viewpoint. However, if we introduce a phonon-frequency-dependent bulk modulus contribution to our system, we would likely see a first order phase transition as we tune the phonon frequency.

The opening of the Mott gap at the Fermi level is present only when the hybridization between conduction band and localized electrons is weak compared with the electron-phonon coupling. Fig. 3 shows that when the hybridization is strong, the opening of the Mott gap is prohibited. In this parameter regime, the introduction of the electron-phonon interaction has little effect on the behavior of the conduction electron DOS. Since the filling number of the c -electrons is set to 0.8, the hybridization cannot induce a gap at the Fermi energy [34], and thus the DOS is always finite irrespective whether there is electron-phonon interaction or not. Consequently, the c -electrons are always metallic in the large V regime.

The absence of the Mott gap in the large V regime signals that the electron-phonon interaction effect is suppressed by the hybridization. Since the electron charge susceptibility is positively correlated with U_{eff} , the suppression of the electron-phonon coupling effect is also reflected in the decrease of the charge susceptibility as V increases for fixed β (not shown). As V increases from 0.1 to 1.8, the localized f electron moments that are present at small V get screened by the conduction electrons when

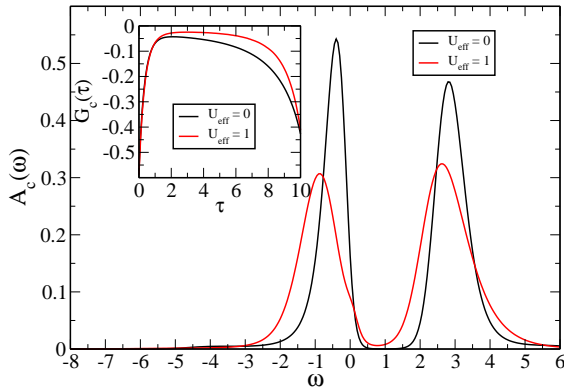


FIG. 3. Main panel: The conduction electrons DOS for $U_{eff} = 0$ and $U_{eff} = 1$ when $V = 1.8, \beta = 10, \Omega_0 = 0.01$. Here, the introduction of the electron-phonon interaction has no significant influence on the DOS, which at the Fermi energy is always finite whether there is electron-phonon interaction or not. Inset: The local $G_c(\tau)$ for small and large electron-phonon interaction strength.

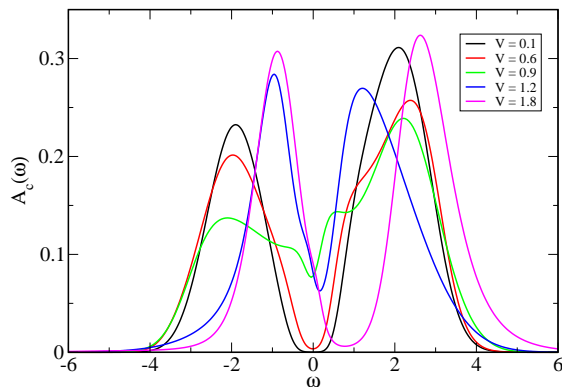


FIG. 4. The c -electron spectral functions for $\beta = 10, \Omega_0 = 0.01, U_{eff} = 1$, at different values of V . When V is small (below 0.6), the electron-phonon interaction dominates over the Kondo screening, and the conduction electrons form a Mott insulator. When V gets large, the Kondo effect dominates over the electron-phonon interaction effect, and the conduction electrons become metallic.

V is large [17]. At the same time, the conduction electrons make a transition from insulator to metal. The c -electron spectral functions for $\beta = 10$ and $U_{eff} = 1$ with varying values of V are shown in Fig. 4, where a gap at the Fermi energy is clearly visible for $V < 0.6$. When $V > 0.6$, the Mott gap evolves into a depression which disappears completely for $V > 1.2$. Therefore the Mott metal-insulator transition is present only when the electron-phonon interaction is strong enough.

In conclusion, using the periodic Anderson model with phonons coupled to the conduction band, and by introducing a volume and temperature dependent bulk modulus contribution to the total pressure, we find a first order phase transition which can be identified as the $\gamma \rightarrow \alpha$ volume collapse transition of Cerium. We find that this phase transition is enhanced by the presence of the electron-phonon interaction which various experiments have shown to play an important role in the volume collapse process. Moreover, we find that our model, although originally conceived with the KVC scenario in mind, exhibits several interesting features of the Mott transition, e.g., a gap at the Fermi energy in the conduction electrons opens at low temperature, and this gap is proportional to the effective electron-phonon interaction, U_{eff} . Our numerical results show that the Mott transition observed in our model is probably continuous within our parameter regime.

Acknowledgements. This material is based upon work supported by the National Science Foundation under the NSF EPSCoR Cooperative Agreement No. EPS-1003897 with additional support from the Louisiana Board of Regents. Computer support is provided by the Louisiana Optical Network Initiative, and by HPC@LSU computing.

-
- [1] A. W. Lawson and T.-Y. Tang, Phys. Rev. **76**, 301 (1949), URL <http://link.aps.org/doi/10.1103/PhysRev.76.301>.
- [2] B. Johansson, Philosophical Magazine **30**, 469 (1974).
- [3] J. W. Allen and R. M. Martin, Phys. Rev. Lett. **49**, 1106 (1982), URL <http://link.aps.org/doi/10.1103/PhysRevLett.49.1106>.

- [4] K. Held, C. Huscroft, R. Scalettar, and A. McMahan, Phys. Rev. Lett. **85**, 373 (2000).
- [5] K. Held, A. McMahan, and R. Scalettar, Phys. Rev. Lett. **87**, 276404 (2001).
- [6] L. Z. Liu, J. W. Allen, O. Gunnarsson, N. E. Christensen, and O. K. Andersen, Phys. Rev. B **45**, 8934 (1992), URL <http://link.aps.org/doi/10.1103/>

- PhysRevB.45.8934.
- [7] A. K. McMahan, K. Held, and R. T. Scalettar, Phys. Rev. B **67**, 075108 (2003), URL <http://link.aps.org/doi/10.1103/PhysRevB.67.075108>.
- [8] A. P. Murani, Z. A. Bowden, A. D. Taylor, R. Osborn, and W. G. Marshall, Phys. Rev. B **48**, 13981 (1993), URL <http://link.aps.org/doi/10.1103/PhysRevB.48.13981>.
- [9] C. R. Burr and S. Ehara, Phys. Rev. **149**, 551 (1966), URL <http://link.aps.org/doi/10.1103/PhysRev.149.551>.
- [10] M. Jarrell, Phys. Rev. Lett. **69**, 168 (1992), URL <http://link.aps.org/doi/10.1103/PhysRevLett.69.168>.
- [11] A. Georges and G. Kotliar, Phys. Rev. B **45**, 6479 (1992), URL <http://link.aps.org/doi/10.1103/PhysRevB.45.6479>.
- [12] T. Pruschke, D. L. Cox, and M. Jarrell, Phys. Rev. B **47**, 3553 (1993), URL <http://link.aps.org/doi/10.1103/PhysRevB.47.3553>.
- [13] F. Decremps, D. Antonangeli, B. Amadon, and G. Schmerber, Phys. Rev. B **80**, 132103 (2009), URL <http://link.aps.org/doi/10.1103/PhysRevB.80.132103>.
- [14] M. Krisch, D. Farber, R. Xu, D. Antonangeli, C. Aracne, A. Beraud, T.-C. Chiang, J. Zarestky, D. Y. Kim, E. I. Isaev, et al., Proceedings of the National Academy of Sciences **108**, 9342 (2011).
- [15] B. Amadon, S. Biermann, A. Georges, and F. Aryasetiawan, Phys. Rev. Lett. **96**, 066402 (2006), URL <http://link.aps.org/doi/10.1103/PhysRevLett.96.066402>.
- [16] I.-K. Jeong, T. W. Darling, M. J. Graf, T. Proffen, R. H. Heffner, Y. Lee, T. Vogt, and J. D. Jorgensen, Phys. Rev. Lett. **92**, 105702 (2004), URL <http://link.aps.org/doi/10.1103/PhysRevLett.92.105702>.
- [17] P. Zhang, P. Reis, K.-M. Tam, M. Jarrell, J. Moreno, F. Assaad, and A. K. McMahan, Phys. Rev. B **87**, 121102 (2013), URL <http://link.aps.org/doi/10.1103/PhysRevB.87.121102>.
- [18] A. Georges, G. Kotliar, W. Krauth, and M. J. Rozenberg, Rev. Mod. Phys. **68**, 13 (1996), URL <http://link.aps.org/doi/10.1103/RevModPhys.68.13>.
- [19] F. F. Assaad and T. C. Lang, Phys. Rev. B **76**, 035116 (2007), URL <http://link.aps.org/doi/10.1103/PhysRevB.76.035116>.
- [20] W. E. Pickett, A. J. Freeman, and D. D. Koelling, Phys. Rev. B **23**, 1266 (1981), URL <http://link.aps.org/doi/10.1103/PhysRevB.23.1266>.
- [21] R. Podloucky and D. Glötzl, Phys. Rev. B **27**, 3390 (1983), URL <http://link.aps.org/doi/10.1103/PhysRevB.27.3390>.
- [22] M. Jarrell and J. E. Gubernatis, Physics Reports **269**, 133 (1996).
- [23] L. de' Medici, A. Georges, G. Kotliar, and S. Biermann, Phys. Rev. Lett. **95**, 066402 (2005), URL <http://link.aps.org/doi/10.1103/PhysRevLett.95.066402>.
- [24] K. Mikelsons, E. Khatami, D. Galanakis, A. Macridin, J. Moreno, and M. Jarrell, Phys. Rev. B **80**, 140505 (2009), URL <http://link.aps.org/doi/10.1103/PhysRevB.80.140505>.
- [25] A. McMahan, C. Huscroft, R. Scalettar, and E. Pollock, Journal of Computer-Aided Materials Design **5**, 131 (1998).
- [26] J. R. Schrieffer and P. A. Wolff, Phys. Rev. **149**, 491 (1966), URL <http://link.aps.org/doi/10.1103/PhysRev.149.491>.
- [27] R. Grover, I. C. Getting, and G. C. Kennedy, Phys. Rev. B **7**, 567 (1973), URL <http://link.aps.org/doi/10.1103/PhysRevB.7.567>.
- [28] F. Murnaghan, Proceedings of the National Academy of Sciences **30**, 244 (1944).
- [29] P. Yu, R. Wang, D. Zhao, and H. Bai, Applied Physics Letters **91**, 201911 (2007).
- [30] D. Meyer, A. Hewson, and R. Bulla, Phys. Rev. Lett. **89**, 196401 (2002).
- [31] Q. Si, G. Kotliar, and A. Georges, Phys. Rev. B **46**, 1261 (1992), URL <https://link.aps.org/doi/10.1103/PhysRevB.46.1261>.
- [32] J. Freericks and V. Zlatić, Reviews of Modern Physics **75**, 1333 (2003).
- [33] E. Müller-Hartmann, Zeitschrift für Physik B Condensed Matter **76**, 211 (1989).
- [34] T. Pruschke, R. Bulla, and M. Jarrell, Phys. Rev. B **61**, 12799 (2000).